Limnol. Oceanogr., 50(5), 2005, 1581–1591

On the role of colloidal particles in light scattering in the ocean

Dariusz Stramski[1]
Marine Physical Laboratory, Scripps Institution of Oceanography, University of California at San Diego, La Jolla, California 92093-0238

Sławomir B. Woźniak
Institute of Oceanology, Polish Academy of Sciences, Powstańców Warszawy 55, 81-712 Sopot, Poland; Marine Physical Laboratory, Scripps Institution of Oceanography, University of California at San Diego, La Jolla, California 92093-0238

Abstract

We calculated the optical scattering and backscattering coefficients for assemblages of marine colloids from the measured size distribution and the assumed refractive index of colloids. The comparison of pure seawater scattering and backscattering coefficients with our results from 11 samples of small colloids (sized between 0.01 and 0.2 μm) and 10 samples of large colloids ($\sim$0.4–1 μm) suggests that (1) the role of colloids in light scattering in the ocean can vary from insignificant to very important as a result of variations in the concentration, size distribution, and refractive index of particles; (2) whereas small colloids generally play an insignificant role in particulate scattering, large colloids can make a sizable contribution because their scattering can exceed that of pure water by more than an order of magnitude; and (3) small colloids appear to play an important role in the overall colloidal backscattering. The combined backscattering of small and large colloids is typically higher than that of pure seawater over most of the visible spectrum (e.g., by a factor of 2.5 at 550 nm and 5.6 at 700 nm from our average results). This indicates that the contribution of colloids to the particulate backscattering is typically significant.

Colloid material is usually defined as microparticles, macromolecules, and molecular assemblies in the size range between 1 nm and 1 μm (Vold and Vold 1983; Buffle and van Leeuwen 1992). The submicrometer-sized particles are the most abundant particles suspended in ocean waters. The concentrations of small colloids ($<$0.2 μm) can exceed 10^{15} m^{-3} (Wells and Goldberg 1991, 1994), which is at least one order of magnitude higher than typical concentrations of viruses that belong to that size range (Bergh et al. 1989; Maranger and Bird 1995). The abundance of larger colloids (sized between $\sim$0.4 and 1 μm) can exceed 10^{13} m^{-3}, which is typically one to two orders of magnitude higher than the number of bacteria within that submicron range (Koike et al. 1990; Longhurst et al. 1992; Yamasaki et al. 1998). These results indicate the dominance of nonliving particles in the submicrometer range.

Marine colloids have received much attention because of their significance in biogeochemical cycling of organic matter and bioactive elements, as well as fate and transport of toxic elements and pollutants (Moran and Moore 1989; Guo et al. 1994; Moran et al. 1996). From a chemical point of view, the functional definition proposes that ''an aquatic colloid is any constituent that provides a molecular milieu into and onto which chemicals can escape from the aqueous solution and whose environmental fate is predominantly affected by coagulation–breakup mechanisms, as opposed to removal by settling'' (Gustafsson and Gschwend 1997, p. 523). Colloidal particles are thus considered to be large enough to possess an interface and interior chemically distinct from the surrounding medium but small enough for gravitational settling to be insignificant. Such a ''chemcentric'' definition allows for discriminating colloids from a truly soluble phase and from settling particles. The colloidal phase consists of a variety of organic microparticles, polymeric organic substances and gels, inorganic particles, organic–inorganic complexes, and living microbes and viruses (Leppard et al. 1997; Chin et al. 1998; Santschi et al. 1998). Because of low electron opacity of most colloids observed by transmission electron microscopy, Wells and Goldberg (1991, 1992) suggested a predominantly organic composition.

The role of marine colloids in light propagation in the ocean is poorly understood. The problems involved in quantifying this role include instrumental and methodological limitations, especially difficulties in accurate determinations of concentration of colloids and their properties. Oceanographers have traditionally used the filtration of water through 0.2- or 0.45-μm pore-size filters to partition water samples into ''dissolved'' and ''particulate'' phases. Interpretation of light absorption by colloids has been confounded by the execution of measurements on the operationally defined dissolved and particulate phases, which both include colloidal particles. Previous efforts to quantify the light scattering by marine colloids have been based mostly on theoretical considerations. Some of these early studies suggested that submicrometer particles can be a significant source of scattering, especially in backscattering directions (Brown and Gordon

[1] Corresponding author (dstramski@ucsd.edu).

Acknowledgments

This study was supported by National Science Foundation grant OCE 04-28900 and National Aeronautics and Space Administration grant NNG04GK50G in the United States. Partial support was also provided by the State Committee for Scientific Research grant PBZ-KBN 056/P04/2001 in Poland. We thank Mark L. Wells and Akiko Yamasaki for providing data of colloidal size distribution, R. Iturriaga and D. Siegel for microspectrophotometric data of detrital particles, and two anonymous reviewers for comments on the manuscript.

1974; Gordon 1974). Calculations of a light-scattering budget associated with various particle types also indicated the significance of colloidal material to backscattering (Morel and Ahn 1991; Stramski and Kiefer 1991). In addition, it was pointed out that at typical particle concentrations in the submicrometer range, the nonliving material appears to be more important to backscattering than viruses and microbes such as bacteria (*see* also Stramski et al. 2004). Laboratory measurements of light scattering by viral suspensions supported the notion that viruses are not a major source of light scattering in ocean waters (Balch et al. 2000).

Light scattering in the ocean is caused by a continuum of particle sizes, so improving our knowledge of scattering contributions by different particle types and size fractions that play different roles in marine biogeochemistry and ecosystems is important (e.g., Stramski et al. 2001). This knowledge is a prerequisite not only to an understanding of substantial variability in optical properties and light fields within the ocean and leaving the ocean but also to applications including satellite remote sensing for estimating water constituents that are biogeochemically important. In that regard, marine colloids represent a particularly interesting size range because they can account for a large fraction (30–50%) of organic carbon within the operationally defined dissolved phase (Benner et al. 1992; Guo et al. 1994). They also show the potential to affect the remote-sensing reflectance of the ocean owing to considerable contribution to light backscatter (Morel and Ahn 1991; Stramski and Kiefer 1991). An important limitation of earlier analyses of colloidal light scattering was the lack of particle size and concentration measurements in the submicrometer size range. Quantifying colloidal scattering without such measurements could involve substantial uncertainty because the particle concentration and size distribution are first-order determinants of the scattering properties of water samples. The objective of this study is to quantify the range of variability in the spectral scattering and backscattering coefficients for assemblages of marine colloids, whose concentrations and size distributions were actually measured in various regions of the world's ocean.

Methods

Our approach involves calculations with Mie scattering theory for homogeneous spherical particles (Mie 1908; Bohren and Huffman 1983). The input data to these calculations include the measured size distributions of marine colloids and the assumed values for the complex index of refraction of particles.

Input data—Our analysis is carried out for two particle size fractions; the small colloids sized between 0.01 and 0.2 μm and the large colloids sized between ~0.4 and 1 μm. We have selected the measured particle size distributions from two studies that cover various oceanic conditions, from nearshore environments with high phytoplankton biomass to oligotrophic open ocean waters. The study by Wells and Goldberg (1994) provided the data for small colloids, and the study by Yamasaki et al. (1998) provided the data for large colloids.

We selected 11 size distributions of small colloids from the data set of Wells and Goldberg (1994) (Fig. 1). Their measurements were made in North Atlantic waters on the Scotian Shelf, the Scotian slope, and in the Sargasso Sea, as well as in shelf and open-ocean waters off the Antarctic Peninsula in the Southern Ocean. We use the data collected within the top 50 m of the ocean (with the exception of one sample from the Sargasso Sea collected at 70 m). Our primary interest in the surface oceanic layer stems from the applicability of optical remote sensing to surface waters and the significance of biological production within the upper water column. Colloid numbers and sizes were determined by Wells and Goldberg (1994) from images of samples, which were obtained with transmission electron microscopy. The detection limit for colloid concentrations was $\sim 10^{13}$ m^{-3}, which corresponded to one to two colloids in a microscope field. Colloid sizes, D, were determined as twice the minor axis of an ellipse having the same area as the colloid. The size distributions of small colloids used in our study are based on colloid counts within 19 size classes, each of which has a width, ΔD, of 0.01 μm. These classes cover a range of sizes between $D_{min} = 0.01$ μm and $D_{max} = 0.2$ μm. Because of incomplete recovery efficiencies of colloids with an ultracentrifugation technique, Wells and Goldberg (1994) indicated that their data should be considered a conservative low estimate of colloid concentrations, especially in the <0.03-μm fraction. In addition, fibrillar colloids (Santschi et al. 1998) were not included in particle counts by Wells and Goldberg (1994).

For large colloids, we used 10 size distributions measured by Yamasaki et al. (1998) in northwest Pacific coastal environments (Fig. 2). Water samples from four stations along a nearshore–offshore transect from the Sagami Bay to off the Izu Islands (Japan) were analyzed. The measurements were made with an electronic particle counter (Elzone 80XY). With this instrument, the measured particle size, D, represents the volume-equivalent spherical diameter. The size range analyzed was from $D_{min} = 0.425$ μm to $D_{max} = 0.99$ μm. The size distributions are based on particle counts within 34 size classes whose width varies between 0.01 and 0.024 μm. The detection limit of particle concentration was 10^8 m^{-3}.

The size distributions provide the values of $N(D)\Delta D$ for each size class, where $N(D)\Delta D$ is the number of particles per unit volume of water within the size class of width ΔD, and where D is the midpoint of the particle size class. The values of $N(D)\Delta D$ and D are used as inputs to our Mie scattering calculations. A common feature of the distributions shown in Figs. 1 and 2 is a decrease in the particle concentration with increasing D, although some irregularities can be superimposed on this general pattern. The small colloids show significant variability in the concentration of particles and the shape of the size distribution both between and within sampling regions, which includes variation with sampling depth (Fig. 1). In contrast, the large colloids show relatively small differences in the shape of the distribution, although variations in particle concentration are large (Fig. 2).

The complex refractive index of particles is also required as input to Mie calculations. To our knowledge, no data exist on the refractive index of marine colloids, so assumptions

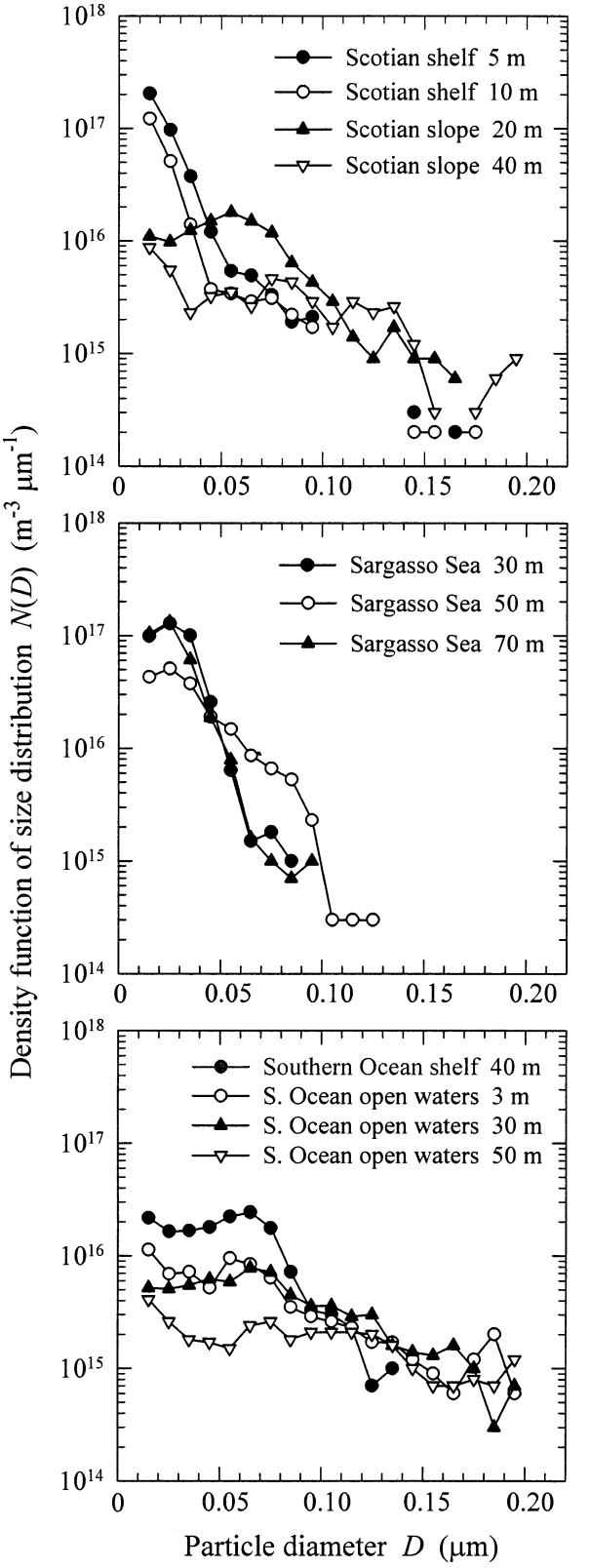

Fig. 1. The density function of particle number size distribution for samples of small colloids obtained from measurements of Wells and Goldberg (1994).

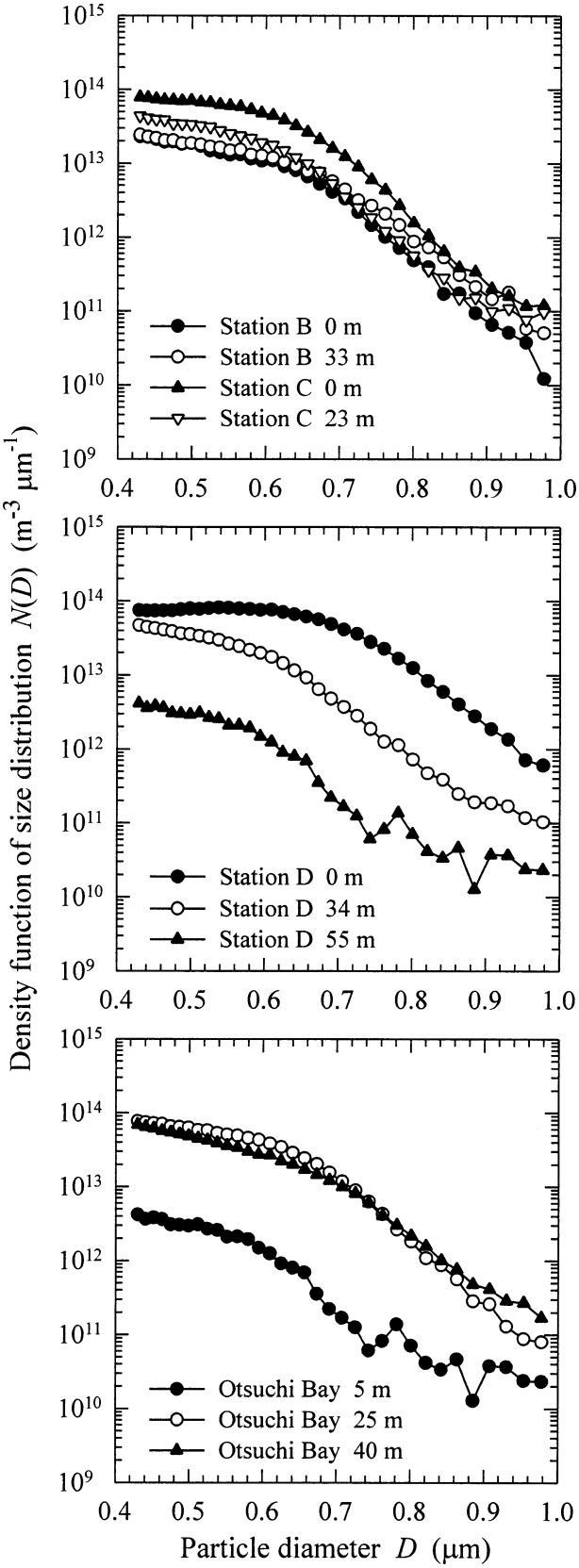

Fig. 2. The density function of particle number size distribution for samples of large colloids obtained from measurements of Yamasaki et al. (1998).

are necessary about the spectral values of the real and imaginary parts of the refractive index of the particles relative to water, $n(\lambda)$ and $n'(\lambda)$, respectively (λ is light wavelength in a vacuum, and we assume that the refractive index of water is 1.34). We chose to make two basic sets of Mie calculations: one for a low value of $n = 1.04$ and the other for a high value of $n = 1.18$. In each case, we assumed that n is independent of λ. The low refractive index is typical for many organic particles that are characterized by relatively high water content. For example, on the basis of metabolite composition and water content of phytoplankton cells, Aas (1996) showed that n of the cells varies typically between 1.02 and 1.08. The high refractive index is typical for mineral particles and dry (or weakly hydrated) organic compounds. For example, the mean n is 1.124 for montmorillonite, 1.155 for crystalline quartz, 1.167 for kaolinite, 1.171 for illite, and 1.195 for calcite (Kerr 1977). The mean n is 1.146–1.167 for dry algal mass, 1.172 ± 0.0075 for protein, and 1.157 ± 0.015 for carbohydrates (Aas 1996). Although it cannot be assumed that all colloids at any given time or location in the ocean have either a low or high refractive index, one could expect that our scattering calculations for $n = 1.04$ and $n = 1.18$ will demonstrate a plausible range of variability associated with colloidal composition. As a sensitivity test, we made additional Mie calculations for a very low value of $n = 1.02$.

Given the lack of data on light absorption by colloids, it is sufficient to our analysis to make a realistic assumption that colloids exhibit some absorption that increases toward the short-wavelength end of the spectrum. Both organic detrital particles and mineral particles typically show two main features: first, a small or undetectable absorption in the red and near-infrared spectral region (Babin and Stramski 2002, 2004), and second, an increase in absorption with decreasing λ, which is often approximated by an exponential function (Bricaud and Stramski 1990; Babin et al. 2003). Figure 3 shows the variation in the imaginary part of the refractive index, n', of marine detrital particles. We determined these n' spectra from an inverse model (Bricaud and Morel 1986) applied to microspectrophotometric measurements of individual particles made by Iturriaga and Siegel (1989) in the Sargasso Sea. They measured particle sizes and absorption efficiency factors at 10 wavelengths (between 410 and 675 nm) for 11 to 35 particles at different depths. The mean particle size ranged from 9 to 27 μm at different depths. For this analysis of colloids, we made Mie calculations with the average spectrum $n'(\lambda)$ (thick solid line in Fig. 3) that was obtained from seven spectral curves (thin solid lines in Fig. 3) corresponding to the Iturriaga and Siegel (1989) samples from depths of 4, 10, 20, 25, 40, 50, and 60 m. The total number of particles analyzed for the average spectrum $n'(\lambda)$ was 143. This spectrum represents a relatively weak particle absorption with $n'(\lambda)$ on the order of 10^{-4}. To test the sensitivity of our colloidal results to changes in $n'(\lambda)$, we made additional Mie calculations for the lowest and the highest $n'(\lambda)$ among the thin solid lines in Fig. 3. These low and high $n'(\lambda)$ spectra differ by a factor of about two from the average spectrum at the short-wavelength end of the spectrum (and less at longer wavelengths). Note that Fig. 3 also shows that $n'(\lambda)$ of detrital particles can occasionally be considerably higher (*see* the dotted lines that represent the Iturriaga and Siegel [1989] samples of detrital particles from depths of 80 and 107 m).

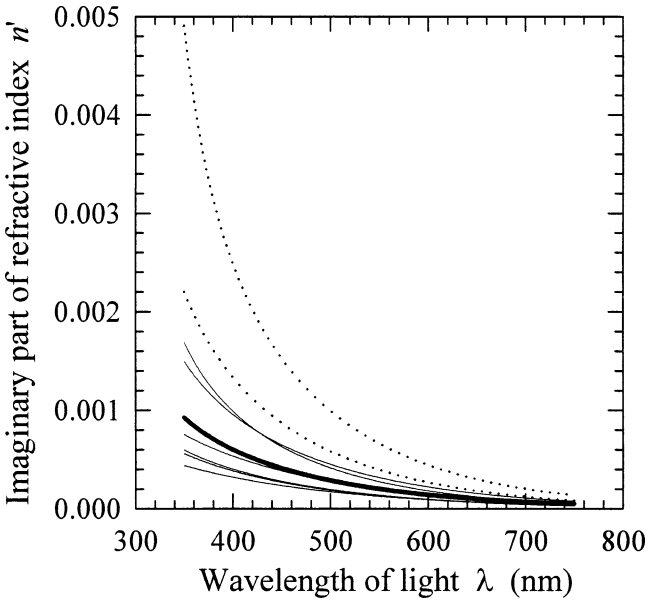

Fig. 3. Spectra of the imaginary part of refractive index (relative to water) of marine detrital particles. Thin solid lines represent exponential fits to n' data obtained at 10 discrete wavelengths between 410 and 675 nm for particles sampled at depths of 4, 10, 20, 25, 40, 50, and 60 m in the Sargasso Sea. The lowest and highest of these curves are for the depths of 10 and 50 m, respectively. Dotted lines are for the depths of 80 and 107 m. The thick solid line is the average spectrum of n' from the data, shown as thin solid lines (one thin solid line is not seen because it is covered by the thick solid line). This average spectrum is assumed in this study for colloids. This spectrum can be described by an exponential function $n'(\lambda) = 0.010658e^{-0.007186\lambda}$.

Calculations of light scattering—We used Mie scattering code for homogeneous spherical particles that allows the calculations to be a function of λ for arbitrary particle size distribution and spectral values of n and n'. The core of the code for a sphere with a given diameter and complex refractive index is published in Bohren and Huffman (1983). The calculations were made for 11 size distributions of small colloids and 10 size distributions of large colloids. For each size distribution, the calculations were made for the assumed values of n and $n'(\lambda)$ (as defined above) in the spectral region from 350 to 750 nm at 1-nm intervals. The assumption that the particles are homogeneous and spherical produces an uncertainty with regard to light scattering by real particles. Most of the colloidal particles analyzed by Wells and Goldberg (1991, 1994) were globular and rounded in shape, and many appeared to be aggregates of smaller granules. However, fibrillar colloids and aggregates of fibrils and globular particles can also be common (Santschi et al. 1998). Presently, it is not possible to evaluate the effect of the inhomogeneous, aggregative, and nonspherical morphology of colloids on their scattering properties.

The quantities obtained with the Mie calculations include the spectral efficiency factors for total scattering, $Q_b(\lambda)$, and

Table 1. Identification of stations where colloidal particles were sampled and the values of the concentration and average projected area of colloidal particles.

Wells and Goldberg (1994) stations	Depth (m)	Total concentration of small colloids N^{SC} (m^{-3})	Average projected areas of small colloids $\bar{G}^{SC}$ (m^2)	Yamasaki et al. (1998) stations	Depth (m)	Total concentration of large colloids N^{LC} (m^{-3})	Average projected areas of large colloids $\bar{G}^{LC}$ (m^2)
Scotian shelf	5	3.68×10^{15}	6.03×10^{-16}	Sta. B	0	3.84×10^{12}	2.34×10^{-13}
	10	2.05×10^{15}	6.54×10^{-16}		33	4.32×10^{12}	2.44×10^{-13}
Scotian slope	20	1.13×10^{15}	3.31×10^{-15}	Sta. C	0	1.53×10^{13}	2.37×10^{-13}
	40	5.04×10^{14}	5.55×10^{-15}		23	6.81×10^{12}	2.27×10^{-13}
Sargasso Sea	30	3.65×10^{15}	6.98×10^{-16}	Sta. D	0	2.32×10^{13}	2.78×10^{-13}
	50	1.89×10^{15}	1.31×10^{-15}		34	7.13×10^{12}	2.25×10^{-13}
	70	3.28×10^{15}	6.45×10^{-16}		55	5.84×10^{11}	2.21×10^{-13}
Southern Ocean shelf	40	1.55×10^{15}	2.62×10^{-15}	Otsuchi Bay	5	2.42×10^{13}	2.72×10^{-13}
Southern Ocean open waters	3	7.61×10^{14}	5.01×10^{-15}		25	1.39×10^{13}	2.37×10^{-13}
	30	6.84×10^{14}	5.81×10^{-15}		40	1.08×10^{13}	2.37×10^{-13}
	50	3.35×10^{14}	7.78×10^{-15}				

backscattering, $\bar{Q}_{bb}(\lambda)$. The efficiency factor $\bar{Q}_b(\lambda)$ at wavelength λ is a ratio of radiant power (at λ) scattered in all directions by a single ''average'' particle derived from the examined polydisperse particulate assemblage to the radiant power (at λ) incident on the geometric cross-section, $\bar{G}$, of the ''average'' particle. The definition of $\bar{Q}_{bb}(\lambda)$ is similar but involves only backward scattering angles. For a given size distribution and complex refractive index of particles, $\bar{Q}_b(\lambda)$ and $\bar{Q}_{bb}(\lambda)$ are calculated from Eq. 1 (Bricaud and Morel 1986; Morel and Bricaud 1986),

$$\bar{Q}_i(\lambda) = \frac{\int_{D_{min}}^{D_{max}} Q_i(\lambda, D, n, n')N(D)D^2\, dD}{\int_{D_{min}}^{D_{max}} N(D)D^2\, dD} \quad (1)$$

where the subscript i is used to denote either b or bb; $Q_i(\lambda, D, n, n')$ is the efficiency factor at λ calculated from the Mie theory for a particle that has a diameter D, the real part of the refractive index relative to water, n, and the imaginary part of the relative refractive index, n' (both n and n' are at wavelength λ); and $N(D)$ is the density function of the size distribution (i.e., the number of particles within the size class centered at D per unit volume of water and per unit width of the size class). An ultimate objective of our calculations was to estimate the scattering, $b(\lambda)$, and backscattering, $b_b(\lambda)$, coefficients (m^{-1}), which are produced by a population of colloidal particles that obey a given size distribution $N(D)$. The coefficient $b(\lambda)$ was obtained from

$$b(\lambda) = \bar{Q}_b(\lambda)\bar{G}\int_{D_{min}}^{D_{max}} N(D)\, dD \quad (2)$$

where $\int_{D_{min}}^{D_{max}} N(D)\, dD$ is the total number of particles in the size range from D_{min} to D_{max} per unit volume of water (for brevity, this total particle concentration will be denoted by N), and $\bar{G}$ is determined by Eq. 3.

$$\bar{G} = \frac{\frac{\pi}{4}\int_{D_{min}}^{D_{max}} N(D)D^2\, dD}{\int_{D_{min}}^{D_{max}} N(D)\, dD} \quad (3)$$

The backscattering coefficient $b_b(\lambda)$ was obtained from Eq. 4.

$$b_b(\lambda) = \bar{Q}_{bb}(\lambda)\bar{G}N \quad (4)$$

We also calculated the backscattering ratio $\tilde{b}_b(\lambda) = \bar{Q}_{bb}(\lambda)/\bar{Q}_b(\lambda)$—equivalently, $b_b(\lambda)/b(\lambda)$—which is a measure of the contribution of backscattering to total scattering.

Results and discussion

Concentration and size of colloids—Table 1 summarizes the data of N and $\bar{G}$ calculated from the size distributions presented in Figs. 1 and 2. For clarity, in the notation of N and $\bar{G}$, we use the superscript ''SC'' to indicate that the variable represents the small colloids and the superscript ''LC'' to indicate the large colloids. The total concentrations of small colloids were highest in the Scotian Shelf (depth 5 m) and Sargasso Sea (30 m), where N^{SC} exceeded 3.6×10^{15} m^{-3}. The lowest N^{SC} of 3.35×10^{14} m^{-3} was observed in the Southern Ocean (50 m). Thus, N^{SC} varies by an order of magnitude among the samples examined. A similar range of variability (a factor of ~13) is observed for $\bar{G}^{SC}$, which is a measure of variation in the shape of the size distribution. Interestingly, the small colloids show a remarkable tendency; the higher N^{SC} is, the smaller $\bar{G}^{SC}$ is. For example, the sample with the highest N^{SC} (Scotian Shelf, 5 m) has the smallest $\bar{G}^{SC}$ ($=6.03 \times 10^{-16}$ m^2), and the sample with the lowest N^{SC} (Southern Ocean, 50 m) has the largest $\bar{G}^{SC}$ ($=7.78 \times 10^{-15}$ m^2).

The large colloids show large variations in N^{LC} but relatively small variations in the shape of the size distribution, and hence relatively small variations in $\bar{G}^{LC}$ (Table 1). The maximum value of N^{LC} (Otsuchi Bay, 5 m) is ~40 times higher than the minimum value (Sta. D, 55 m). However, there is a difference by a factor of only 1.25 between the

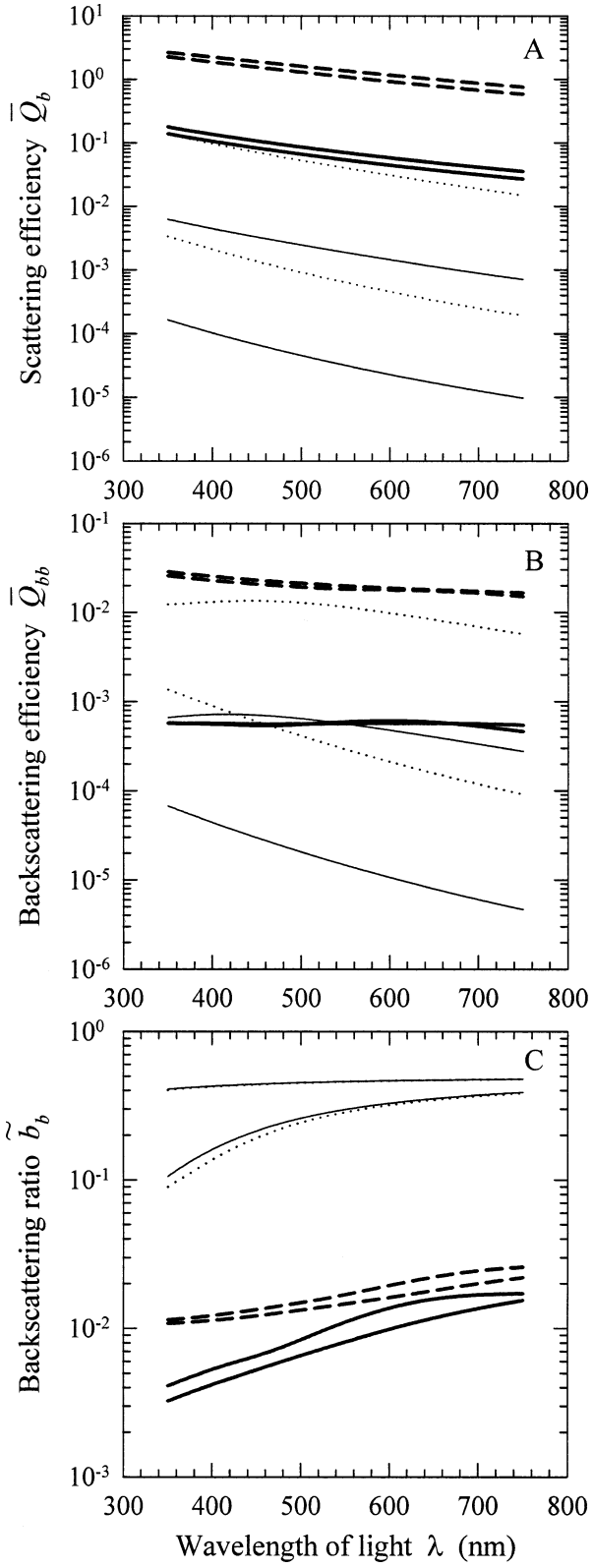

Fig. 4. (A) The range of variation in the scattering efficiency of colloidal particles. Thin solid lines show the minimum $\bar{Q}_b(\lambda)$ (Sargasso Sea, 30 m) and maximum $\bar{Q}_b(\lambda)$ (Southern Ocean, 50 m) for small colloids with a particle refractive index of $n = 1.04$ relative to water. Dotted lines correspond to the same two samples of small colloids but with $n = 1.18$. Thick solid lines show the minimum and maximum values of $\bar{G}^{LC}$ (*see* Sta. D, 0 m and 55 m, in Table 1). The result, that the shape of the size distribution of large colloids is weakly variable, is intriguing, but it is based on 10 samples from one region only. Further scrutiny of this question is required.

The product $N \times G$ represents the total projected area of suspended particles per unit volume of water. The average value of $N^{SC} \times G^{SC}$ from all samples of small colloids is 2.88 m^{-1}, which is similar to the average value of $N^{LC} \times G^{LC} = 2.77$ m^{-1} for large colloids. However, the variability among the samples is much smaller for $N^{SC} \times G^{SC}$ than for $N^{LC} \times G^{LC}$. Whereas the minimum and maximum of $N^{SC} \times G^{SC}$ are 1.34 m^{-1} and 4.06 m^{-1}, respectively, there is a 50-fold difference between the minimum (0.13 m^{-1}) and maximum (6.58 m^{-1}) of $N^{LC} \times G^{LC}$. The small range of $N^{SC} \times G^{SC}$ is caused by the inverse relationship between N^{SC} and G^{SC}. The large variation in $N^{LC} \times G^{LC}$ is associated primarily with variation in N^{LC}.

Optical properties derived from Mie calculations—The efficiency factors $Q_b(\lambda)$ and $Q_{bb}(\lambda)$ of colloids are shown in Fig. 4A,B, respectively. To illustrate the range of variation, only the lowest and highest spectral curves among the samples examined are displayed. For small colloids, both Q factors show large variation. For a given value of n, the Sargasso Sea sample (30 m) shows the lowest $Q_b(\lambda)$ and $Q_{bb}(\lambda)$, and the Southern Ocean sample (50 m) shows the highest values. This is attributable to the effect of particle size distribution because in the size range of small colloids, both efficiency factors increase rapidly with an increase in particle size (Bricaud and Morel 1986; Morel and Bricaud 1986). The Sargasso Sea sample (30 m) shows steep size distribution and relatively small G^{SC}; hence, $Q_b(\lambda)$ and $Q_{bb}(\lambda)$ are low. Because the slope of size distribution for the Southern Ocean sample (50 m) is less steep and G^{SC} is larger, $Q_b(\lambda)$ and $Q_{bb}(\lambda)$ are much higher. The difference in $Q_b(\lambda)$ between these extreme samples is a factor of ~40 at 350 nm, 60 at 550 nm, and almost 80 at 750 nm. For $Q_{bb}(\lambda)$, the difference is a factor of 10 at 350 nm, 40 at 550 nm, and 60 at 750 nm. The extent of this particle size–induced variation in $Q_b(\lambda)$ and $Q_{bb}(\lambda)$ is similar regardless of whether $n = 1.04$ or 1.18. However, for any sample of small colloids, the increase of n from 1.04 to 1.18 produces an ~20-fold increase in $Q_b(\lambda)$ and $Q_{bb}(\lambda)$. Note that the lowest values of $Q_b(\lambda)$ or $Q_{bb}(\lambda)$ calculated with $n = 1.18$ for the Sargasso Sea sample are comparable to the highest $Q_b(\lambda)$ or $Q_{bb}(\lambda)$ calculated with $n = 1.04$ for the Southern Ocean sample.

Because of the effect of particle size on efficiency factors (e.g., Bricaud and Morel 1986), the $Q_b(\lambda)$ and $Q_{bb}(\lambda)$ values for large colloids are higher than those for small colloids. However, there is little variation in $Q_b(\lambda)$ and $Q_{bb}(\lambda)$ among

←

imum $\bar{Q}_b(\lambda)$ (Station D, 55 m) and maximum $\bar{Q}_b(\lambda)$ (Station D, 0 m) for large colloids with $n = 1.04$. Thick dashed lines correspond to the same two samples of large colloids but with $n = 1.18$. (B) Same as panel A, but the spectra represent the backscattering efficiency factor. (C) Same as panel A, but the spectra represent the backscattering ratio.

the different samples of large colloids at a given refractive index (Figs. 4A,B). This is a result of small changes in the shape of the particle size distribution of large colloids. The differences in $Q_b(\lambda)$ are 15–30% between the extreme samples (Sta. D, 0 and 55 m). The variation in $Q_{bb}(\lambda)$ is even smaller, generally <10%. The effect of n on $Q_b(\lambda)$ and $Q_{bb}(\lambda)$ of large colloids is strong. The increase of n from 1.04 to 1.18 induces a 15- to 20-fold increase in $Q_b(\lambda)$ and a 30- to 50-fold increase in $Q_{bb}(\lambda)$.

The angular distribution of scattered light is expected to vary considerably as a function of colloid size because small colloids are smaller than the wavelength of light and large colloids are comparable or somewhat larger than λ (e.g., Morel and Bricaud 1986). The backscattering ratio, $\tilde{b}_b(\lambda)$, reflects these changes (Fig. 4C). For the small colloids, $\tilde{b}_b(\lambda)$ is relatively large and ranges from ~0.1 to 0.5, the latter value being a limit representing molecular scattering with equal forward and backward scattering. The highest $\tilde{b}_b(\lambda)$ was obtained for the Sargasso Sea sample (30 m), for which $\tilde{b}_b(\lambda)$ increases from ~0.4 at 350 nm to 0.48 at 750 nm. For the large colloids, $\tilde{b}_b(\lambda)$ is significantly lower, ranging from ~0.003 to 0.025. These values indicate forward-dominated scattering. Whereas the values of $\tilde{b}_b(\lambda)$ for small colloids are weakly dependent on n, the increase of n produces a substantial enhancement of $\tilde{b}_b(\lambda)$ for large colloids. Both the small and large colloids are characterized by an increase of $\tilde{b}_b(\lambda)$ with λ.

Bulk scattering and backscattering coefficients—The range of variation in $b(\lambda)$ and $b_b(\lambda)$ is illustrated in Figs. 5, 6 for small and large colloids, respectively. According to Eqs. 2 and 4, $b(\lambda)$ or $b_b(\lambda)$ is controlled by the product of three variables: N, G, and $Q_b(\lambda)$ or $Q_{bb}(\lambda)$. For the small colloids, the Southern Ocean sample (3 m) shows the highest values of $b(\lambda)$ and $b_b(\lambda)$ (Fig. 5). The Southern Ocean (30 and 50 m) and the Scotian Slope (40 m) samples also exhibited relatively high $b(\lambda)$ and $b_b(\lambda)$ (not shown). These high values of $b(\lambda)$ and $b_b(\lambda)$ were obtained despite the lowest particle concentrations in these samples (N^{SC} on the order of 10^{14} m^{-3}; *see Table 1*). For these samples, the low N^{SC} is compensated for by the highest values of $G^{SC} > 5 \times 10^{-15}$ m^2 (Table 1) and the highest values of $Q_b(\lambda)$ and $Q_{bb}(\lambda)$. The Sargasso Sea samples (70 and 30 m) show by far the lowest $b(\lambda)$ and $b_b(\lambda)$. Although N^{SC} for these samples is relatively high ($>3 \times 10^{15}$ m^{-3}), G^{SC} and Q factors are relatively small. Our general observation for small colloids is that the large variations in $Q_b(\lambda)$ and $Q_{bb}(\lambda)$ associated with changes in the size distribution counteract the inverse relationship between N^{SC} and G^{SC} to the extent that $b(\lambda)$ and $b_b(\lambda)$ exhibit large variation among the samples examined. For example, for $n = 1.04$ and $\lambda = 550$ nm, $b(550)$ varies between 8.07×10^{-5} m^{-1} (Sargasso Sea, 70 m) and 6.02×10^{-3} m^{-1} (Southern Ocean, 3 m), which represents a 75-fold change. The $b_b(550)$ coefficient varies between 3.71×10^{-5} m^{-1} (Sargasso Sea, 70 m) and 1.82×10^{-3} m^{-1} (Southern Ocean, 3 m), which represents a 50-fold change.

To gain more insight into the potential role of small colloids in light scattering in the ocean, our results in Fig. 5 are compared with the scattering and backscattering coefficients of pure seawater, $b_w(\lambda)$ and $b_{bw}(\lambda)$. It is well recognized that $b_w(\lambda)$ makes only a small contribution (typically <10%) to the total scattering coefficient of seawater, even in clearest ocean waters. However, $b_{bw}(\lambda)$ can make a large or even dominant contribution to the total backscattering coefficient in clear ocean waters; typically tens of a percent and, in extreme cases, up to ~80% in the blue spectral region (Morel and Gentili 1991). The coefficients $b_w(\lambda)$ and $b_{bw}(\lambda)$ show strong wavelength dependence of $\lambda^{-4.32}$. In the middle of the spectrum at $\lambda = 550$ nm, the generally ac-

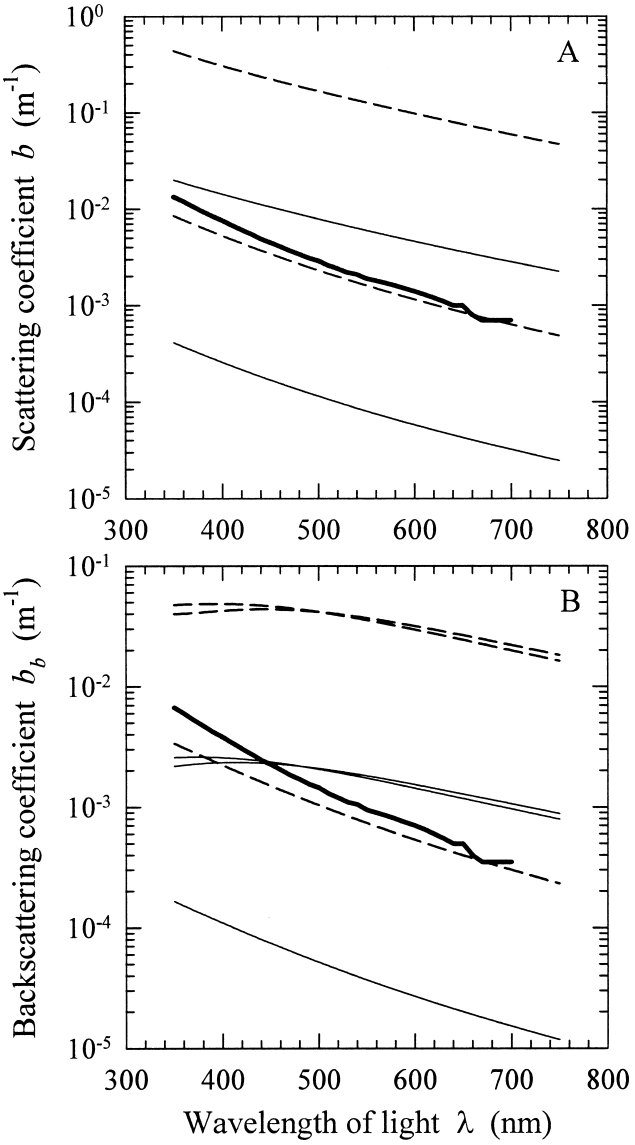

Fig. 5. (A) The range of variation in the scattering coefficient of small colloids. Thin solid lines show the minimum $b(\lambda)$ (Sargasso Sea, 70 m) and maximum $b(\lambda)$ (Southern Ocean, 3 m) for small colloids with $n = 1.04$. Dashed lines correspond to the same two samples of small colloids but with $n = 1.18$. For comparison, the scattering spectrum of pure seawater is also shown (thick solid line). (B) Same as panel A, but the spectra represent the backscattering coefficient. The minimum $b_b(\lambda)$ corresponds to the sample from the Sargasso Sea (70 m). Two curves representing the maximum $b_b(\lambda)$ are displayed (Southern Ocean, 3 and 30 m). These two samples show very similar $b_b(\lambda)$.

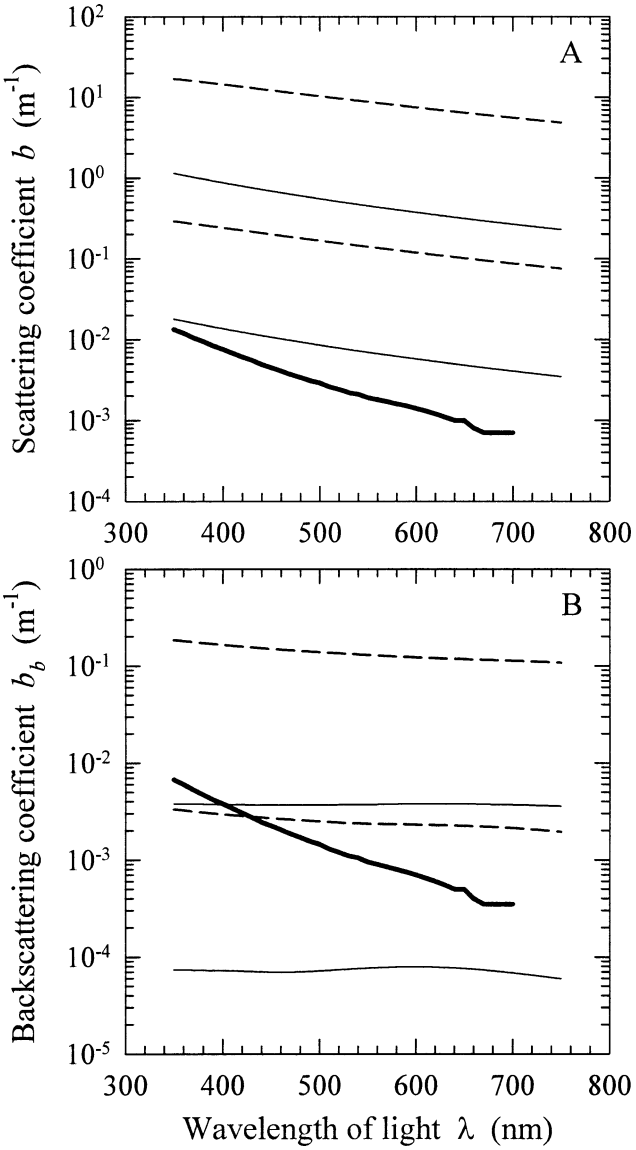

Fig. 6. The range of variation in the scattering coefficient of large colloids. Thin solid lines show the minimum $b(\lambda)$ (Sta. D, 55 m) and maximum $b(\lambda)$ (Sta. D, 0 m) for large colloids with $n = 1.04$. Dashed lines correspond to the same two samples of large colloids but with $n = 1.18$. For comparison, the scattering spectrum of pure seawater is also shown (thick solid line). (B) Same as panel A, but the spectra represent the backscattering coefficient. The minimum $b_b(\lambda)$ corresponds to the sample from Sta. D (55 m) and the maximum $b_b(\lambda)$ to the sample from Otsuchi Bay (5 m).

cepted scattering and backscattering values are $b_w(550) = 0.0019$ m^{-1} and $b_{bw}(550) = 0.00095$ m^{-1} (Morel 1974; Smith and Baker 1981).

We take a closer look at the comparison of $b_w(\lambda)$ and $b_{bw}(\lambda)$, with conservative estimates for small colloids (i.e., for $n = 1.04$). As seen in Fig. 5, $b_w(\lambda)$ and $b_{bw}(\lambda)$ generally fall within the range of variation of $b(\lambda)$ and $b_b(\lambda)$ of the low-index small colloids. The Southern Ocean sample (3 m) produces $b(550)$ that is over three times higher than $b_w(550)$, and it produces $b_b(550)$ that is nearly twice as high as $b_{bw}(550)$. These results suggest that the contribution of small colloids to the total scattering and backscattering coefficients of seawater can be important in some situations. Our analysis cannot, however, answer the question of how widespread such conditions are in the ocean. Our results also suggest that scenarios with a negligible role of small colloids are likely to occur, as indicated by the lowest curves for low-index small colloids in Fig. 5. Specifically, the calculations for the Sargasso Sea sample (70 m) with $n = 1.04$ produce $b(\lambda)$ and $b_b(\lambda)$ that are lower than $b_w(\lambda)$ and $b_{bw}(\lambda)$ by a factor of ~25.

The results for small colloids with $n = 1.18$ in Fig. 5 show that an increase of n from 1.04 to 1.18 produces a 20-fold increase in $b(\lambda)$ and $b_b(\lambda)$, just as for $Q_b(\lambda)$ and $Q_{bb}(\lambda)$. If all the small colloids had $n = 1.18$ (which is naturally unrealistic), $b(550)$ would be as high as 0.127 m^{-1} and $b_b(550)$ would be as high as 3.68×10^{-2} m^{-1}, as indicated by the calculations for the Southern Ocean sample (3 m). These values are improbably high. Circumstantial evidence for this conclusion is provided by determinations of the total particulate backscattering coefficient, b_{bp}, from in situ measurements in the Southern Ocean (Stramski et al. 1999; Reynolds et al. 2001). Those measurements showed b_{bp} on the order of 10^{-4}–10^{-3} m^{-1} in the green spectral region. Our calculations for a low refractive index produce more realistic results (than those for the high index) in the sense that the calculated values are not higher than the typical estimates of particulate scattering or backscattering from measurements in the ocean. Nevertheless, one must bear in mind that some colloids likely have a high refractive index, which will enhance scattering compared with the scenario in which all colloids have a low refractive index.

Figure 6 shows $b(\lambda)$ and $b_b(\lambda)$ for large colloids. As for the small colloids, the use of the high refractive index for large colloids appears to produce unrealistically high values of $b(\lambda)$ and $b_b(\lambda)$. This is indicated by the high values of $b_b(\lambda)$ for $n = 1.18$, which in extreme cases extend above 0.1 m^{-1}. For a given sample of large colloids, the $b(\lambda)$ and $b_b(\lambda)$ values for $n = 1.18$ are higher by 20- and 50-fold, respectively, than those for $n = 1.04$.

There is a large variation in $b(\lambda)$ and $b_b(\lambda)$ among the samples of large colloids (Fig. 6). For $n = 1.04$, we found a 65-fold range in $b(\lambda)$ and a 50- to 60-fold range in $b_b(\lambda)$ between the samples with the highest scattering (Otsuchi Bay, 5 m) and the lowest scattering (Sta. D, 55 m). This variation is driven primarily by changes in the total concentration of large colloids, N^{LC}. Recall that N^{LC} for Otsuchi Bay (5 m) is ~40 times higher than that for Sta. D (55 m; Table 1). The remaining part of the variation in $b(\lambda)$ and $b_b(\lambda)$ is attributable to relatively small differences in the values of G^{LC} and efficiency factors $Q_b(\lambda)$ and $Q_{bb}(\lambda)$, which are associated with relatively small variations in the shape of the size distribution of large colloids.

The importance of large colloids to total $b(\lambda)$ and $b_b(\lambda)$ in the ocean is suggested on the basis of the comparison with pure seawater curves in Fig. 6. The calculations for $n = 1.04$ produced colloidal $b(\lambda)$ that is higher than $b_w(\lambda)$ for all samples examined. For all but one sample (Sta. D, 55 m), $b(\lambda)$ is at least an order of magnitude higher than $b_w(\lambda)$. The range of $b_b(\lambda)$ for $n = 1.04$ generally encompasses the range associated with spectral variation of $b_{bw}(\lambda)$ (Fig. 6B). The

lowest curve for Sta. D (55 m) is distinctive in the sense that $b_b(\lambda)$ is much lower than that of all the remaining samples examined. The second lowest $b_b(\lambda)$ (Sta. B, 33 m; not shown) is ~8 times higher than that for Sta. D (55 m). As a result, all samples of large colloids except for Sta. D (55 m) have $b_b(\lambda)$ higher than $b_{bw}(\lambda)$ in the red portion of the spectrum.

The spectral shape of $b(\lambda)$ and $b_b(\lambda)$ of colloids is the same as that for $Q_b(\lambda)$ and $Q_{bb}(\lambda)$ (*see Eqs. 2, 4*). For the small colloids, the best fit values of the exponent γ of the power function $b(\lambda) \sim \lambda^{-\gamma}$ range from 2.9 to 3.8 among the different samples (not shown). The effect of n on γ is very small (<2%). The slope χ of the power function $b_b(\lambda) \sim \lambda^{-\chi}$ varies between 1.1 and 3.6. For the Southern Ocean samples (*see* the highest $b_b(\lambda)$ in Fig. 5B), the spectra of $b_b(\lambda)$ flatten noticeably in the blue-violet spectral region. For these particular spectra, the power function fit over the entire wavelength range of 350–750 nm is not appropriate. The slope γ of large colloids is less steep and more sensitive to n than that for small colloids. For the large colloids, γ ranges from 2.15 for the calculations with $n = 1.04$ to 1.7–1.8 for $n = 1.18$. The backscattering spectra $b_b(\lambda)$ of large colloids with $n = 1.04$ are nearly flat, with only slight undulation within the spectrum. For $n = 1.18$, the slope χ ranges between 0.6 and 0.7 for different samples.

To assess the sensitivity of our findings to assumptions, we made three types of additional calculations. First, we tested the sensitivity to the real part of the refractive index, n. Specifically, the sensitivity calculations showed that $b(\lambda)$ and $b_b(\lambda)$ of colloids with a very low refractive index of $n = 1.02$ are reduced to ~25% of the values calculated for $n = 1.04$. Second, we tested the sensitivity to the imaginary part of the refractive index, n' (i.e., the absorption of light by colloids). The calculations with n' that differ by as much as a factor of about two at the short wavelength end of the spectrum from our base average n' showed a negligible effect on colloidal scattering. The largest difference between our base calculations and the sensitivity calculations was ~1.3% for backscattering by large colloids at short wavelengths. Finally, we tested the assumption about the absolute accuracy of the size distribution data for small colloids. These colloids were examined with electron microscopy techniques (Wells and Goldberg 1994), which can result in particle shrinkage (e.g., Montesinos et al. 1983). We tentatively assumed that the original particle sizes reported by Wells and Goldberg are underestimated by 20% in terms of particle volume. The sensitivity calculations with the modified size distributions of small colloids produced the scattering coefficients 30–40% higher and the backscattering coefficients 10–40% higher than those obtained with the original size distributions.

Given the possible range of variability in the colloidal concentration, size distribution, and optical properties, it is difficult to draw simple generalized conclusions about the role of colloids in light scattering in the ocean. The collection of colloid size distribution data used in this study was not accompanied by light scattering measurements. Therefore, our calculations of colloidal scattering cannot be compared with the total particulate scattering by the samples examined, so we cannot estimate the contribution of colloids to light scattering for these samples. The comparison of our calculations with pure seawater scattering and backscattering coefficients provides, however, insights into the potential role of colloids. The results suggest that this role could be quite variable and often times highly significant. On averaging the data for colloids with $n = 1.04$ (i.e., quite conservative estimates with respect to the refractive index), we find that the average scattering coefficient of small colloids from the 11 samples examined is comparable to the scattering coefficient of pure seawater (Fig. 7A). The latter is known to be generally much smaller than the total particulate scattering. The average scattering of large colloids from the 10 samples examined is more than an order of magnitude

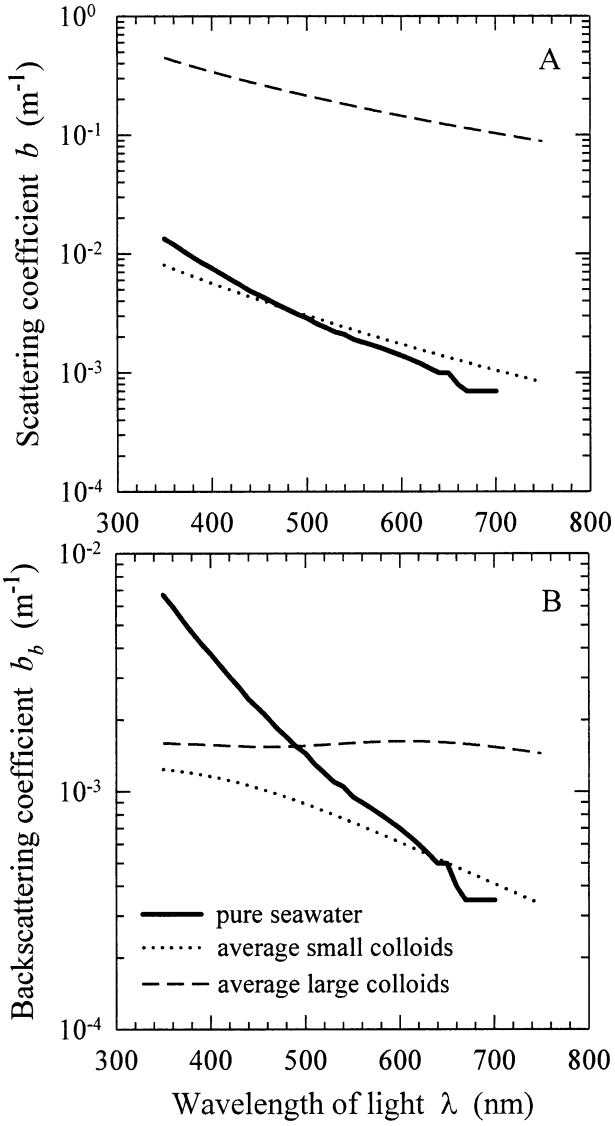

Fig. 7. (A) Spectra of the scattering coefficient of colloidal particles as calculated by averaging the results for the 11 examined samples of small colloids with the refractive index $n = 1.04$ (dotted line) and by averaging the results for the 10 examined samples of large colloids with $n = 1.04$ (dashed line). For comparison, the spectrum for pure seawater is shown (thick solid line). (B) Same as panel A, but the spectra represent the backscattering coefficient.

higher than pure seawater scattering. It thus appears that, whereas small colloids play a generally small or insignificant role in total particulate scattering, large colloids can make a substantial contribution. In any particular situation, this contribution will, however, depend also on the role of larger particles (>1 μm) present in water.

The average backscattering of small colloids from the 11 samples (with $n = 1.04$) is comparable to pure seawater backscattering in the red portion of the spectrum, but in the blue, the pure seawater values are considerably higher (Fig. 7B). For the large colloids, the average backscattering spectrum is quite flat, with the values higher than pure seawater at $\lambda > 500$ nm but lower at shorter λ. Because water molecules are an important contributor to the total backscattering in natural waters that are not very turbid (such as the open ocean), Fig. 7B suggests that the colloidal contribution to the particulate backscattering can be significant or dominant. If we add the average backscattering values for small and large colloids, the result is higher than pure water backscattering over most of the visible region (with the exception of the shortest wavelengths), for example, by a factor of 2.5 at 550 nm and 5.6 at 700 nm. The small colloids contribute 44% at 350 nm and 19% at 750 nm to this average total colloidal backscattering.

A key benefit of this study over previous calculations of colloidal scattering is the use of actual measurements of colloid concentration and size distribution in seawater. Although this approach provided estimates of the potential range of colloid scattering in the ocean, significant knowledge gaps remain with respect to quantifying the colloid contributions to the scattering and backscattering coefficients in various environmental situations. Mie scattering calculations with a homogeneous sphere model are certainly an oversimplification, but attempts to quantify colloidal scattering with more complex modeling would still be fraught with uncertainty that is difficult to assess. Current limitations in modeling result from the inability to characterize the real heterogeneous particle assemblages in terms of all particle properties that govern scattering, such as size, shape, complex refractive index, internal structures, and degree of aggregation, for example.

Further advancements in understanding the role of colloids in the optical properties of aquatic environments are needed, especially because of the potential broader influences beyond the field of optics. For example, an adequate knowledge of the optical signature of colloids such as backscattering could lead to new optical methods for measuring colloid-related biogeochemical properties over extended temporal and spatial scales. It seems that the greatest promise for acquiring such knowledge lies in developing observation strategies and methods for parallel optical measurements and characterization of submicron particles.

References

AAS, E. 1996. Refractive index of phytoplankton derived from its metabolite composition. J. Plankton Res. **18:** 2223–2249.

BABIN, M., AND D. STRAMSKI. 2002. Light absorption by aquatic particles in the near-infrared spectral region. Limnol. Oceanogr. **47:** 911–915.

———, AND ———. 2004. Variations in the mass-specific absorption coefficient of mineral particles suspended in water. Limnol. Oceanogr. **49:** 756–767.

———, ———, G. M. FERRARI, H. CLAUSTRE, A. BRICAUD, G. OBOLENSKY, AND N. HOEPFFNER. 2003. Variations in the light absorption coefficients of phytoplankton, non-algal particles, and dissolved organic matter in coastal waters around Europe. J. Geophys. Res. **108**(C7). [doi: 10.1029/2001JC000882]

BALCH, W. M., J. VAUGHN, J. NOVOTNY, D. T. DRAPEAU, R. VAILLANCOURT, J. LAPIERRE, AND A. ASHE. 2000. Light scattering by viral suspensions. Limnol. Oceanogr. **45:** 492–498.

BENNER, R., J. D. PAKULSKI, M. MCCARTHY, J. I. HEDGES, AND P. G. HATCHER. 1992. Bulk chemical characteristics of dissolved organic matter in the ocean. Science **255:** 1561–1564.

BERGH, Ø., K. Y. BØRSHEIM, G. BRATBAK, AND M. HELDAL. 1989. High abundance of viruses found in aquatic environments. Nature **340:** 467–468.

BOHREN, C. F., AND D. R. HUFFMAN. 1983. Absorption and scattering of light by small particles. J. Wiley.

BRICAUD, A., AND A. MOREL. 1986. Light attenuation and scattering by phytoplanktonic cells: A theoretical modeling. Appl. Opt. **25:** 571–580.

———, AND D. STRAMSKI. 1990. Spectral absorption coefficients of living phytoplankton and non-algal biogenous matter: A comparison between the Peru upwelling area and Sargasso Sea. Limnol. Oceanogr. **35:** 562–582.

BROWN, O. B., AND H. R. GORDON. 1974. Size-refractive index distribution of clear coastal water particulates from light scattering. Appl. Opt. **13:** 2874–2881.

BUFFLE, J., AND H. P. VAN LEEUWEN [EDS.]. 1992. Environmental particles. V. 1. Lewis.

CHIN, W.-C., M. V. ORELLANA, AND P. VERDUGO. 1998. Spontaneous assembly of marine dissolved organic matter into polymer gels. Nature **391:** 568–572.

GORDON, H. R. 1974. Mie-theory models of light scattering by ocean particulates, p. 73–86. *In* J. R. Gibbs [ed.], Suspended solids in water. Plenum Press.

GUO, L., C. H. COLEMAN, JR., AND P. H. SANTSCHI. 1994. The distribution of colloidal and dissolved organic carbon in the Gulf of Mexico. Mar. Chem. **45:** 105–119.

GUSTAFSSON, Ö., AND P. M. GSCHWEND. 1997. Aquatic colloids: Concepts, definitions, and current challenges. Limnol. Oceanogr. **42:** 519–528.

ITURRIAGA, R., AND D. A. SIEGEL. 1989. Microspectrophotometric characterization of phytoplankton and detrital absorption properties in the Sargasso Sea. Limnol. Oceanogr. **34:** 1706–1726.

KERR, P. F. 1977. Optical mineralogy, 4th ed. McGraw-Hill.

KOIKE, I., S. HARA, K. TERAUCHI, AND K. KOGURE. 1990. Role of sub-micrometre particles in the ocean. Nature **345:** 242–244.

LEPPARD, G. G., M. M. WEST, D. T. FLANNINGAN, J. CARSON, AND J. N. A. LOTT. 1997. A classification scheme for marine organic colloids in the Adriatic Sea: Colloid speciation by transmission electron microscopy. Can. J. Fish. Aquat. Sci. **54:** 2334–2349.

LONGHURST, A. R., AND OTHERS. 1992. Sub-micron particles in northwest Atlantic shelf water. Deep-Sea Res. **39:** 1–7.

MARANGER, R., AND D. F. BIRD. 1995. Viral abundance in aquatic systems: A comparison between marine and fresh waters. Mar. Ecol. Prog. Ser. **121:** 217–226.

MIE, G. 1908. Beiträge zur Optik trüber Medien, speziell kolloidaler Metallösungen. Ann. Phys. **25:** 377–445.

MONTESINOS, E., I. ESTEVE, AND R. GUERRERO. 1983. Comparison between direct methods for determination of microbial cell volume: Electron microscopy and electronic particle sizing. Appl. Environ. Microbiol. **45:** 1651–1658.

MORAN, S. B., AND R. M. MOORE. 1989. The distribution of col-

loidal aluminum and organic carbon in coastal and open ocean waters off Nova Scotia. Geochim. Cosmochim. Acta **53:** 2519–2527.

———, P. A. YEATS, AND P. W. BALLS. 1996. On the role of colloids in trace metals solid-solution partitioning in continental shelf waters: A comparison of model results and field data. Cont. Shelf Res. **16:** 397–408.

MOREL, A. 1974. Optical properties of pure water and pure sea water, p. 1–24. *In* N. G. Jerlov and E. Steeman-Nielsen [eds.], Optical aspects of oceanography. Academic Press.

———, AND Y.-H. AHN. 1991. Optics of heterotrophic nanoflagellates and ciliates. A tentative assessment of their scattering role in oceanic waters compared to those of bacterial and algal cells. J. Mar. Res. **49:** 177–202.

———, AND A. BRICAUD. 1986. Inherent optical properties of algal cells including picoplankton: Theoretical and experimental results, p. 521–559. *In* T. Platt and W. K. W. Li [eds.], Photosynthetic picoplankton. Can. Bull. Fish. Aquat. Sci. **214.**

———, AND B. GENTILI. 1991. Diffuse reflectance of oceanic waters: Its dependence on sun angle as influenced by the molecular scattering contribution. Appl. Opt. **30:** 4427–4438.

REYNOLDS, R. A., D. STRAMSKI, AND B. G. MITCHELL. 2001. A chlorophyll-dependent semianalytical reflectance model derived from field measurements of absorption and backscattering coefficients within the Southern Ocean. J. Geophys. Res. **106:** 7125–7138.

SANTSCHI, P. H., E. BALNOIS, K. J. WILKINSON, J. ZHANG, AND J. BUFFLE. 1998. Fibrillar polysaccharides in marine macromolecular organic matter as imaged by atomic force microscopy and transmission electron microscopy. Limnol. Oceanogr. **43:** 896–908.

SMITH, R. C., AND K. BAKER. 1981. Optical properties of the clearest natural waters. Appl. Opt. **20:** 177–184.

STRAMSKI, D., E. BOSS, D. BOGUCKI, AND K. J. VOSS. 2004. The role of seawater constituents in light backscattering in the ocean. Prog. Oceanogr. **61:** 27–56.

———, A. BRICAUD, AND A. MOREL. 2001. Modeling the inherent optical properties of the ocean based on the detailed composition of planktonic community. Appl. Opt. **40:** 2929–2945.

———, AND D. A. KIEFER. 1991. Light scattering by microorganisms in the open ocean. Prog. Oceanogr. **28:** 343–383.

———, R. A. REYNOLDS, M. KAHRU, AND B. G. MITCHELL. 1999. Estimation of particulate organic carbon in the ocean from satellite remote sensing. Science **285:** 239–242.

VOLD, R. D., AND M. J. VOLD. 1983. Colloid and interface chemistry. Addison-Wesley.

WELLS, M. L., AND E. D. GOLDBERG. 1991. Occurrence of small colloids in sea water. Nature **353:** 342–344.

———, AND ———. 1992. Marine sub-micron particles. Mar. Chem. **40:** 5–18.

———, AND ———. 1994. The distribution of colloids in the North Atlantic and Southern Oceans. Limnol. Oceanogr. **39:** 286–302.

YAMASAKI, A., H. FUKUDA, R. FUKUDA, T. MIYAJIMA, T. NAGATA, H. OGAWA, AND I. KOIKE. 1998. Submicrometer particles in northwest Pacific coastal environments: Abundance, size distribution, and biological origins. Limnol. Oceanogr. **43:** 536–542.

Received: 20 December 2004
Accepted: 27 April 2005
Amended: 28 April 2005